ELSEVIER

Polymer 40 (1999) 7089–7107

polymer

Fracture characterization of PC/ABS blends: effect of reactive compatibilization, ABS type and rubber concentration

G. Wildes, H. Keskkula, D.R. Paul*

Department of Chemical Engineering and Center for Polymer Research, The University of Texas at Austin, Austin, TX 78712, USA

Received 5 January 1998; accepted 12 August 1998

Abstract

The fracture of thin (3.18 mm) and thick (6.35 mm) specimens of polycarbonate (PC), acrylonitrile–butadiene–styrene (ABS) and PC/ABS blends with both standard and sharp notches was examined by standard Izod and single edge notch three point bend (SEN3PB) instrumented Dynatup tests. Ligament lengths were varied for SEN3PB samples and the corresponding fracture data were represented by plotting the specific fracture energy (U/A) as a function of ligament length (ℓ). The slope of these plots was found to be closely related to both the Izod impact strength and the size of the process (or stress whitened) zones surrounding the crack surface. Significant morphology coarsening was seen in some PC/ABS (70/30) blends for thick (6.35 mm) injection molded parts; blends compatibilized with 1% of an SAN-amine polymer exhibited well-dispersed, stable morphologies. The effects of blend composition, ABS type, sample geometry, PC molecular weight, temperature, rubber concentration and reactive compatibilization on the fracture properties of these materials were examined.

Keywords: Polycarbonate; Acrylonitrile–butadiene–styrene; Acrylate–styrene–acrylonitrile

1. Introduction

The commercial success of blends of polycarbonate (PC) with acrylonitrile–butadiene–styrene (ABS) materials is caused by a combination of factors such as improved processability relative to PC and high fracture toughness in the presence of sharp cracks, in thick sections and at low temperatures [1–15]. It is useful to characterize the fracture performance of PC/ABS blends in some detail. The theory of linear elastic fracture mechanics (LEFM) restricts analysis to materials with only small-scale yielding near the crack-tip. Because the plastic zone size is significantly larger than the size of test specimens in ductile engineering polymers, measurement of meaningful K_{1c} values is often not realistic for such materials. Traditionally, the fracture performance of engineering polymer blends has been characterized by the Charpy or Izod tests. Although Izod testing with a single ligament size offers a simple and convenient method for comparing many materials, the fracture characterization of toughened polymers with varying ligament sizes offers a more thorough description of the crack formation and propagation behavior of these materials. Many recent articles have shown the benefits of analysis of fracture data using a two parameter model, which analyzes the fracture energy per unit area as a function of the ligament size [10,16–26]. The use of this type of analysis has provided effective characterization of toughened polymer blends in previous reports from this laboratory [27,28]. Use of thick samples with sharp notches under impact loading conditions offers severe test conditions which better differentiate between super tough polymeric materials that may have very similar Izod impact values. This article examines the effects of reactive compatibilization, blend composition, sample geometry, temperature, and rubber concentration on the fracture properties of PC/ABS blends.

2. Analysis of fracture data with varying ligament size

Two mathematical approaches for analyzing fracture behavior as a function of ligament size were introduced. Each is based on the idea first introduced by Broberg that the region at the tip of a crack consists of an end region where actual fracture occurs and an outer region where energy is plastically absorbed during crack propagation [29].

The essential work of fracture (EWF) method is based on the partitioning of the fracture energy of ductile materials

* Corresponding author. Tel.: + 1-512-471-5392; fax: + 1-512-471-0542.

E-mail address: paul@che.utexas.edu (D.R. Paul)

0032-3861/99/$ - see front matter
PII: S0032-3861(98)00865-9

Table 1
Test conditions and sample geometry for various fracture methods

Test	Test method	Test velocity	Stress condition	t (mm)	W (mm)	Z (mm)	Ligament $\ell = W - a$ (mm)
EWF	SENT, DENT-Tensile (razor notch)	1.7×10^{-5} m/s	Plane stress	1.6	25 (25–50)	58 (20–70)	5–45; (0.2–0.9)W
Izod	Cantilever-impact (standard notch)	3.5 m/s	Plane stress–strain	3.2	12.7	62	10.2; 0.8W
Vu Khanh	SEN3PB-impact (razor notch)	2.5, 3.0 m/s	Plane stress–strain	3–6	10, 12	50, 90	2–10; (0.2–0.8)W
This study	SEN3PB–impact (razor notch)	3.5 m/s	Plane stress–strain	3.2, 6.4	12.7	5.4	2–10; (0.2–0.8)W

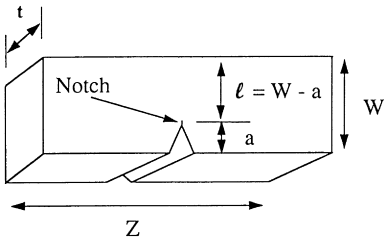

Fig. 1. Schematic of test specimen geometry; values used in this study and in the essential work of fracture, Izod, and Vu Khanh methods are given in Table 1.

into two components, the essential and non-EWF, as proposed by Mai and coworkers [16,21,30,31]. The essential work (W_e) is related to the formation and localized deformation associated with crack extension, while the non-essential work term (W_p) incorporates the plastic work in the volume surrounding the crack region. The sum of these two terms gives the total work of fracture (W_f).

$$W_f = W_e + W_p. \tag{1}$$

For a given sample thickness, t, W_e is proportional to the ligament length, ℓ and W_p has a volumetric dependence and is therefore proportional to ℓ^2

$$W_f = \ell t w_e + \ell^2 t \beta w_p, \tag{2}$$

where β is the plastic zone volumetric shape factor. The specific EWF (energy per unit area) is $w_e = W_e/\ell t$ while $w_p = W_p/\ell^2 t\beta$ is the specific non-EWF (energy per unit volume) equivalent to the energy dissipated in the plastic zone. Therefore, a normalized expression for the total specific work of fracture, w_f, is as follows:

$$w_f = w_e + \beta w_p \ell. \tag{3}$$

Thus, a plot of w_f versus ℓ should give a linear relationship where the intercept at zero ligament length is w_e and the slope is βw_p. For PC, w_e has been experimentally shown to be independent of notch geometry, specimen width, and specimen length [17].

The fracture energy, U, of ductile materials with varying ligament sizes has been proposed by Vu Khanh [24–26] to follow a relationship of the form

$$U = G_i A + 1/2 T_a A^2, \tag{4}$$

where $A = \ell t$ is the area of the ligament. The intercept of a plot of U/A versus A or G_i was called the fracture energy at crack initiation while the term T_a related to the slope was called a tearing modulus or the rate of change of G_r (defined as $G_i + T_a A$) with crack extension.

In addition to the differences in interpretation of the slope and intercepts of these similar linear plots, there are differences in the method of loading, sample geometry, and testing rate in the approaches used by Mai et al. and Vu Khanh. Table 1 compares typical testing parameters and sample geometries from the literature for the two methodologies; sample geometry is schematically shown in Fig. 1. It should be emphasized that while there are similarities in the mathematical analysis of the data obtained from these tests, the actual test conditions are very different; the EWF method uses very thin specimens which are tested at low rates in uniaxial tension, while Vu-Khanh's methodology employs high speed loading of relatively thick specimens in bending which induces a triaxial stress state in the material. Clearly the fracture characterization of toughened polymers with varying ligament sizes offers a more thorough description of the crack formation and propagation behavior of these materials compared to Izod testing which uses a single ligament size.

Many recent articles have shown the benefits of analysis of fracture data using a two-parameter model

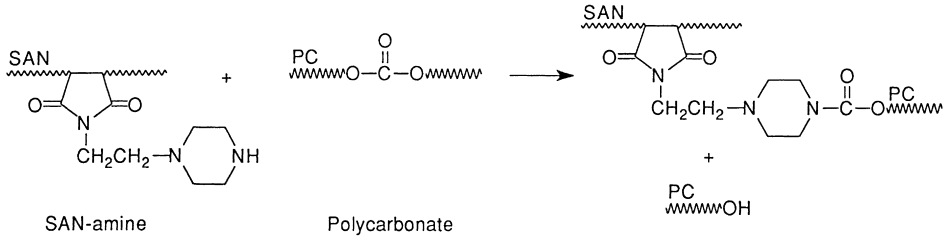

Fig. 2. Schematic of the reaction of SAN-amine with bisphenol-A-polycarbonate to form SAN-g-PC[42].

Table 2
PC and SAN materials used in this study

Polymer	Designation	Description	$\bar{M}_w$	$\bar{M}_n$	Torque (N m)[a]	Relative melt viscosity	Source
Caliber 200-3	VH-PC	BPA polycarbonate Very high MW	36 000	13 400	16.8	0.17	Dow Chemical Company
Iupilon-E2000 H-PC		BPA polycarbonate High MW	32 000	10 800	13.1	0.23	Mitsubishi Engineering Plastics Corporation
Iupilon-S3000 M-PC		BPA polycarbonate Medium MW	23 700	8500	7.7	0.39	Mitsubishi Engineering Plastics Corporation
Iupilon-H3000	L-PC	BPA polycarbonate Low MW	20 100	7400	4.6	0.65	Mitsubishi Engineering Plastics Corporation
Lustran 35	SAN32.5	Styrene acrylonitrile copolymer, 32.5% AN	130 000	59 000	3.00	1.00	Bayer Corporation
Tyril 1000	SAN25	Styrene acrylonitrile copolymer, 25% AN	152 000	77 000	3.6	0.83	Dow Chemical Company
SAN-amine	SAN-amine	Amine functional S/AN/amine (67/32/1)	117 300	48 100	3.8	0.79	Bayer Corporation

[a] Brabender torque taken after 10 min mixing at 270°C and 60 rpm.

Table 3
ABS and ASA materials used in this study

Polymer	Designation	Description	Soluble SAN		Torque (N m)[a]	Source
			$\bar{M}_w$	$\bar{M}_n$		
Magnum541	ABS16	16% Rubber 25% AN in SAN	140 000	59 000	3.9	Dow Chemical Company
Lustran38	ABS38	38% Rubber 30% AN in SAN	130 000	59 000	10.0	Bayer Corporation
SAN-g	ABS45	45% Rubber 25% AN in SAN	90 000	35 000	12.7	Cheil Industries
BL65	ABS50	50% Rubber 24% AN in SAN	167 000	44 000	12.8	Sumitomo Naugatuck Corporation
Geloy	ASA46	46% Acrylate rubber 33% AN in SAN	NA		9.6	GE Plastics

[a] Brabender torque taken after 10 min mixing at 270°C and 60 rpm.

[10,17,18,21,26–28,30]. This study uses thick specimens with sharp notches at high rates of loading in order to better discern between super tough PC/ABS blends and elucidate the importance of constituent materials and morphologies on the fracture performance of these materials. As will be shown, the specific fracture energy of the materials used in this study is more closely a function of ligament length than area. By plotting the normalized fracture energy as a function of ligament length, it is recognized that the intercept and slope may not be equal to w_e and βw_p since the test conditions and sample geometries employed do not conform exactly to the yielding criterion required in the EWF analysis. Therefore, we have defined the intercept, $u_0 \equiv \lim_{\ell \to 0}(U/A)$, simply as the limiting specific fracture energy, and the slope, $u_d = d(U/A)/d\ell$, as the dissipative energy density in the following relationship

$$U/A = u_0 + u_d \ell, \tag{5}$$

where u_d has units of energy/volume and it presumably reflects plastic deformation energy in the process (or stress whitened) zone surrounding the fracture surface. This analysis method is introduced as an adaptation of the EWF concept to facilitate the performance evaluation of super tough blends with thick parts and at high speeds.

3. Compatibilization of PC/ABS using SAN-amine

Reactive compatibilization of polymer blends by the in situ formation of block or graft copolymers reduces

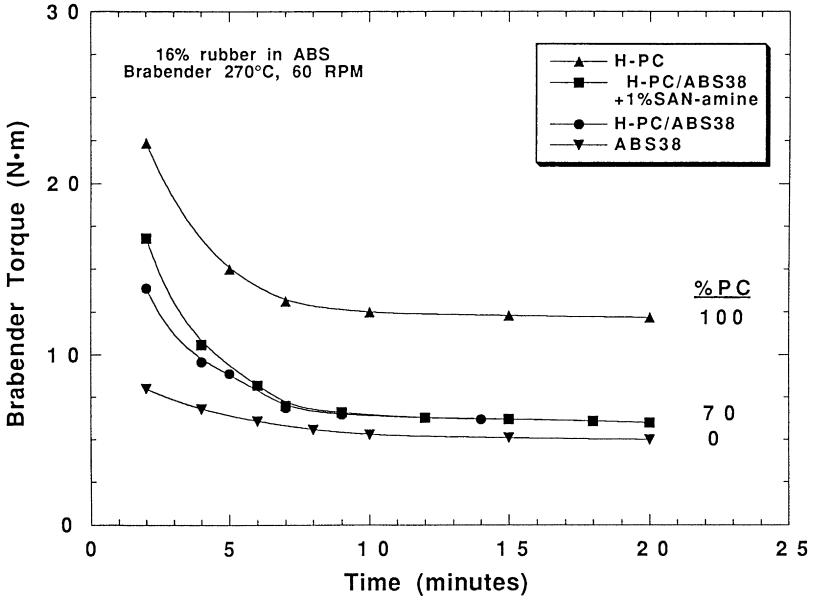

Fig. 3. Brabender torque versus time for H-PC, ABS38, and H-PC/ABS38 (70/30) blends with and without SAN-amine compatibilizer mixed at 270°C and a rotor speed of 60 rpm (16% rubber in ABS phase).

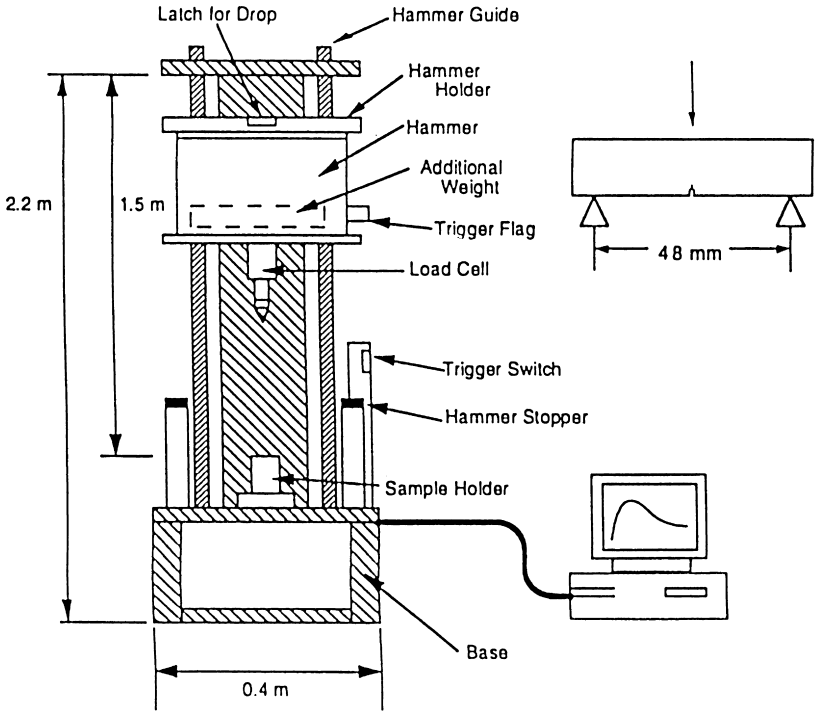

Fig. 4. Schematic of Dynatup single edge notch three point bend (SEN3PB) experimental configuration (10 kg tup at a test velocity of 3.5 m/s) [28].

interfacial tension, introduces a steric hindrance to coalescence and can improve the interfacial adhesion between phases. Chemical schemes for the compatibilization of polyamide blends using maleated rubber modifiers are well known [32–41]; however, the absence of functional chain ends on PC does not provide a straightforward route for compatibilization of its blends. The formation of SAN-g-PC copolymer at the PC/SAN interface is accomplished through the chemical scheme shown in Fig. 2 [42]. The SAN-amine polymer is synthesized by reacting a styrene/acrylonitrile/maleic anhydride (67/32/1) terpolymer with 1-(2-aminoethyl) piperazine in a reactive processing scheme. The SAN-amine polymer is miscible with the SAN matrix of ABS and reacts with PC as shown. The graft copolymer formed was shown to reduce the SAN dispersed phase particle size for different blend compositions, AN contents of the SAN, PC molecular weights and processing conditions [42–44]. The purpose here is to examine the effects of reactive compatibilization on the morphology dependent fracture properties of PC/ABS blends.

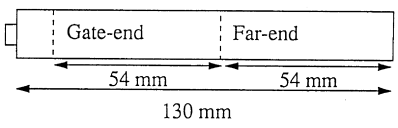

Fig. 5. Schematic of injection molded fracture bar indicating gate and far end fracture specimens; thicknesses of 3.18 mm and 6.35 mm were used.

4. Experimental

4.1. Materials

Details of the PC and SAN polymers employed in this article are shown in Table 2. The designation for each commercial PC is based on its relative molecular weight; e.g., very high molecular weight polycarbonate (VH-PC). Commercial SAN copolymers containing 32.5% AN (SAN32.5) and 25% AN (SAN25) were used; the functionalized SAN-amine polymer was described in a previous article [42]. Table 3 describes the characteristics and suppliers of the ABS and the acrylate–styrene–acrylonitrile (ASA) materials used in this article; each is designated by the type of material followed by its as-received rubber phase concentration. The ABS and ASA materials employed in this article represent different rubber concentrations (16%–45%), AN contents (24%–32%), rubber types (acrylate- and butadiene-based elastomers), and manufacturing processes (bulk and emulsion polymerization). All materials were dried in a vacuum oven at 80°C for at least 12 h before melt processing. Fig. 3 shows Brabender torque as a function of time for H-PC, ABS38 diluted to 16% rubber, and 70/30 blends of these materials with and without 1% SAN-amine. As seen in Fig. 3, the melt viscosity of PC/ABS blends can be significantly lower than for PC which is an important processing advantage of these materials.

Blends were prepared by melt mixing at 40 rpm in a Killion single screw extruder ($L/D = 30$, 25.4 mm diameter)

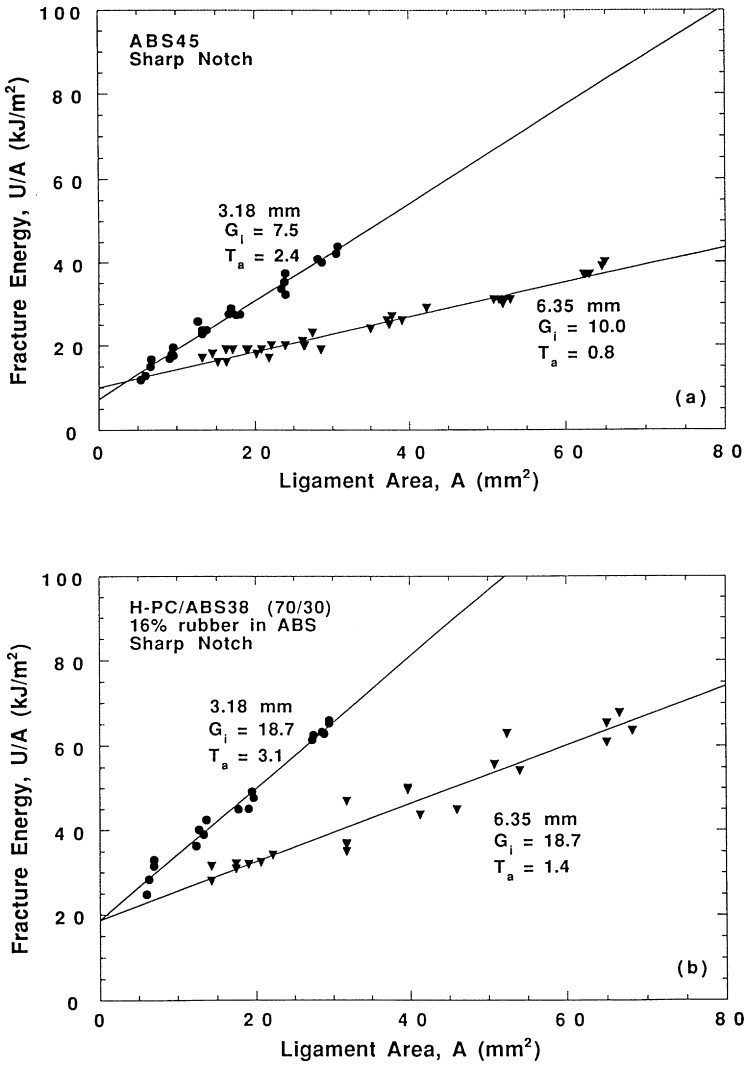

Fig. 6. Fracture energy as a function of ligament area for (a) ABS45 (45% rubber) and (b) H-PC/ABS38 (70/30) with 16% rubber in the ABS phase for thin (3.18 mm) and thick (6.35 mm) samples with a sharp notch.

outfitted with an intensive mixing head. Low rubber content ABS materials were made by blending virgin ABS with SAN25 or SAN32.5, corresponding to the AN content of the ABS material to be diluted. The ABS pellets of reduced rubber concentration were then molded into test specimens or blended with PC. PC/ABS blends were prepared by blending PC with either a virgin ABS or a diluted ABS. ABS materials were processed at 200°C while PC/ABS blends were processed at 270°C. There was no significant difference in the morphology or properties of blends prepared by pre-blending compared with those mixed in a one step process. Test specimens for mechanical property evaluation were produced using a 75 ton Arburg Allrounder 305 screw injection molding machine.

Izod impact testing was performed using a TMI 15 J pendulum type tester. The impact strength data represent average values of at least six test specimens. Standard deviations for these data are typically ±5%, but the variability is greater near transition regions. Standard notch test bars (thickness = 3.18 mm) conformed to ASTM D 256. Liquid carbon dioxide was used to cool samples for low temperature impact testing and a thermocouple implanted in a neighboring test specimen was used to monitor the temperature.

4.2. SEN3PB methodology

Instrumented impact tests were made using a Dynatup Drop Tower Model 8200 with a 10 kg weight at a fracture velocity of 3.5 m/s as shown in Fig. 4 [28]. The single notch, three-point bend (SEN3PB) specimen geometry is described in Table 1 and Fig. 1. Between 24 and 36 samples (one half gate-end and one half far-end specimens as shown in Fig. 5) were tested with original ligament lengths between 2 and 10 mm, (0.2–0.8)W. A sharp notch was made by pressing a fresh razor blade cooled in liquid nitrogen into the root of

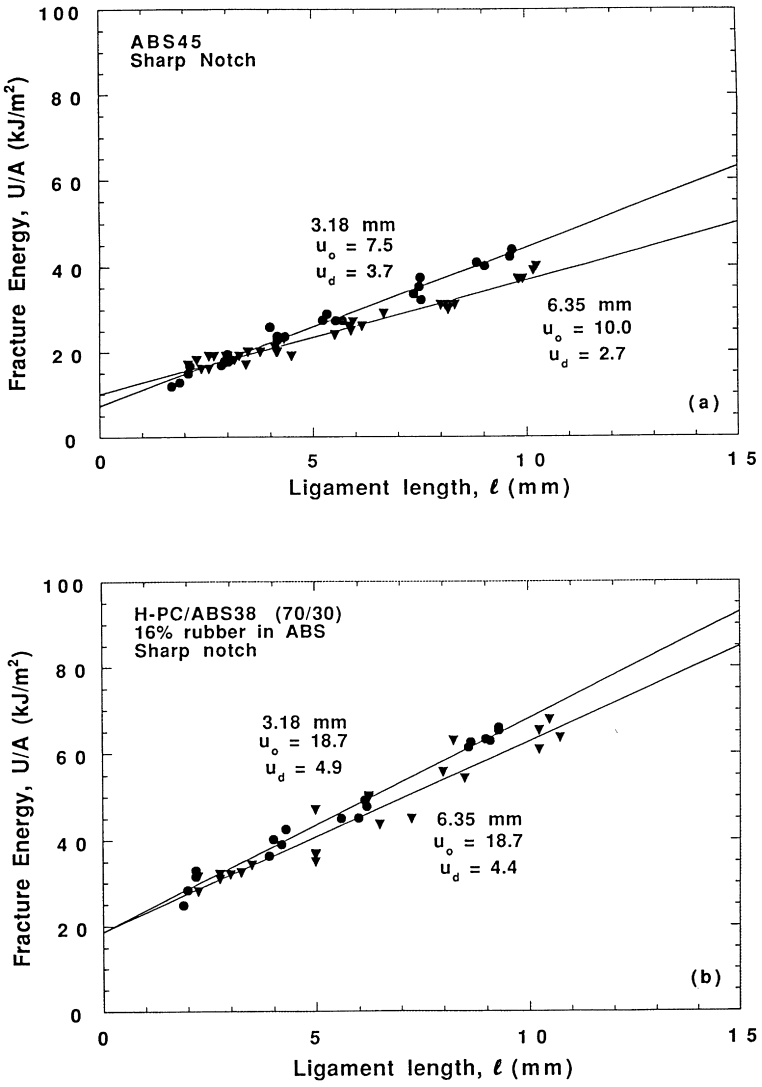

Fig. 7. Fracture energy as a function of ligament length for (a) ABS45 (45% rubber) and (b) H-PC/ABS38 (70/30) with 16% rubber in the ABS phase for thin (3.18 mm) and thick (6.35 mm) samples with a sharp notch.

the notch. Fracture energy was calculated from the integrated area under the load-deflection curves. Although Izod impact testing of these super tough materials resulted in partial breaks with significant unbroken ligaments, Dynatup testing of SEN3PB samples led to complete breaks or hinged ligaments that were generally 0.25 mm or smaller in length. The test apparatus and methodology are described in more detail in previous articles from this research group [27,28].

4.3. TEM analysis

Transmission electron microscopy (TEM) was used to examine the morphology of the melt processed blends of PC/ABS and PC/ABS/SAN-amine. Injection molded specimens were microtomed with a diamond knife perpendicular to the plane of flow in the center of the test sample. The cryogenically microtomed sections, about 20 nm thick, were prepared using a Reichert-Jung Ultracut E at a sample temperature of −10°C using a knife temperature of −45°C.

The butadiene rubber phase of the ABS was stained (black in TEM photomicrographs) by exposing microtomed sections to the vapor of a 2.0% aqueous solution of OsO_4 at room temperature for 18 h. The PC phase of the blends was preferentially stained (gray in TEM photomicrographs) by exposing the ultra-thin sections to the vapors of a 0.5% aqueous solution of RuO_4 at room temperature for 9 min after staining with OsO_4. The dual staining technique provides effective contrast between all three phases in the blend: PC, SAN and rubber. Staining with RuO_4 before OsO_4 resulted in poor phase contrast; the presence of RuO_4 seems to reduce the effectiveness of OsO_4 as a staining agent. Blends of PC with ASA were stained in a one step process which provided contrast between all three phases by exposing ultra-thin sections to the vapors of a 0.5% aqueous solution of RuO_4 at room temperature for 8 min. The use of

Table 4
Fracture properties of polycarbonate materials

PC	3.18 mm Specimens			6.35 mm Specimens				
	Standard notch		Sharp notch	Standard notch	Sharp notch			
	Izod impact strength (J/m)	Ductile–brittle transition temperature (°C)	Izod impact strength (J/m)	Izod impact Strength (J/m)	Izod impact strength (J/m)	Ductile–brittle transition temperature (°C)	Plane Strain fracture parameters	
							u_0 (KJ/m^2)	u_d (MJ/m^3)
VH-PC	1000	−42	95	245	50	>60	4.5	0
H-PC	980	−40	90	225	45	>60	4.3	0
M-PC	880	−30	85	200	40	>60	2.5	0
L-PC	790	−10	75	145	30	>60	2.5	0

RuO_4 to stain acrylate-based rubber has been reported elsewhere in the literature [45,46]. TEM imaging was done on a Jeol 200CX microscope operating at 120 keV.

5. Fracture evaluation of PC/ABS blends

5.1. Effect of sample thickness

Fig. 6(a) and (b) show the fracture response as a function of ligament area, $A = \ell t$, for ABS45 and H-PC/ABS38 (70/30) blends at two different sample thickness. These two plots suggest that the intercept u_0 is relatively independent of sample thickness for the test methodology and specimen geometry used in this article. However, as seen in Fig. 6(a), the slope is decreased by a factor of three when the specimen thickness is doubled. Figs. 7(a) and (b) show that plots of fracture energy versus ligament length, $\ell = W - a$, rather than area result in a slope that is relatively independent of sample thickness compared to plots of fracture energy as a function of ligament area. This suggests that the fracture energy for these materials and testing conditions is more truly a function of ligament length than ligament area.

5.2. Effect of PC molecular weight

The fracture characteristics of the PC materials used in this article are given in Table 4. Increased PC molecular weight results in higher impact strength for 3.18 mm and 6.35 mm specimens with both standard and sharp notches. Thin (3.18 mm) samples with a standard notch are super tough at room temperature while all samples with a sharp notch have Izod impact strengths less than 100 J/m. Thick specimens (6.35 mm) failed in a brittle manner for both standard and sharp notch samples; samples with standard notches exhibited Izod impact strengths approximately five times higher than those with sharp notches. The fracture surface of thick specimens showed that samples with standard notches had a larger rough area near the original crack tip; the greater surface roughness could account for the higher impact energies observed. The limiting specific fracture energy, u_0, and the dissipative energy density, u_d, were calculated by plotting U/A as a function of ligament length for specimens 6.35 mm thick. All four PC materials resulted in plots of U/A versus ℓ with zero slope, i.e. $u_d = 0$; u_0 ranged from 4.5 for the highest molecular weight to 2.5 kJ/m^2 for the lowest molecular weight PC.

The values of u_0 obtained here are similar to related parameters reported in other studies; Paton and Hashemi [17] reported a plane-strain specific work of fracture of 3 kJ/m^2 and a specific work of fracture initiation of 4.3 kJ/m^2 using the EWF method. Plati and Williams [47], and later Singh and Parihar [48], reported values of 4.8 and 6.13 kJ/m^2, respectively using the J-integral technique. Each of these testing methods characterizes the plane-strain fracture response of materials; therefore, calculations were done to confirm that the tests described in this article were

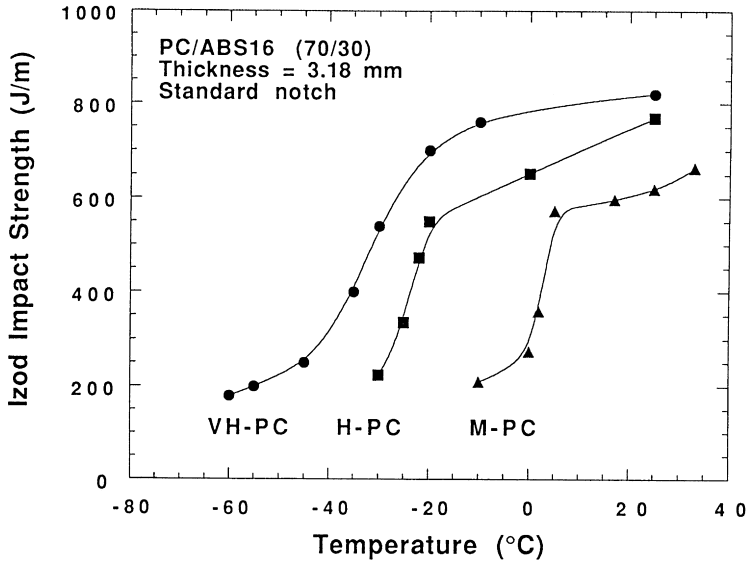

Fig. 8. Izod impact strength of PC/ABS16 (70/30) blends as a function of temperature for VH-PC, H-PC and M-PC using thin (3.18 mm) samples with a standard notch.

also done under plane-strain conditions. The load versus time data from the Dynatup was used to estimate the strain rate during testing, approximately 150 s^{-1}; the effective yield stress $\sigma_y = 79$ MPa at this rate was calculated using an Eyring plot for PC [49]. Using a published value of the stress intensity factor of $K_{1c} = 2.24$ MPa $m^{1/2}$ from Ref. [50], the minimum specimen thickness defined by

$$t_{min} = 2.5(K_{1c}/\sigma_y)^2 \quad (6)$$

for plane-strain fracture conditions as recommended by ASTM is calculated to be approximately 2 mm. Thus, the use of the 6.35 mm specimen thickness assures plane-strain fracture for PC as used in this article.

Fig. 8 shows the Izod impact strength of PC/ABS16 (70/30) blends with three different PCs as a function of temperature using thin (3.18 mm) samples with a standard notch. As seen in Fig. 8, higher PC molecular weights lead to higher impact strengths and lower ductile–brittle transition temperatures in these blends. Although the impact strength of the neat PC materials was higher than the corresponding PC/ABS16 (70/30) blend for thin (3.18 mm) samples, all PCs were brittle in thick (6.35 mm) sections while the blends were tough. H-PC was chosen for all further blend studies because of its combination of low temperature toughness and lower melt viscosity compared to VH-PC.

5.3. Effect of ABS material on PC/ABS blend properties

Table 5 shows the impact fracture characteristics of the

Table 5
Fracture property comparison of ABS and ASA materials

	3.18 mm	6.35 mm		
	Standard notch	Standard notch	Sharp notch	
			Plane strain fracture parameters	
Polymer	Izod impact strength (J/m)	Izod impact strength (J/m)	u_0 (KJ/m^2)	u_d (MJ/m^3)
ABS16	340	235	22	0
ABS38	540	270	15.5	1.0
ABS45	550	340	10.0	2.7
ASA46	540	340	16.6	1.9
ABS50	520	340	10.2	2.6
ABS16[a]		235	22	0
ABS38[a]		65	6.8	0
ABS45[a]		80	8.6	0
ASA46[a]		85	8.9	0

[a] Properties of the ABS or ASA materials indicated after blending with appropriate SAN copolymers to obtain a final rubber content of 16% by weight.

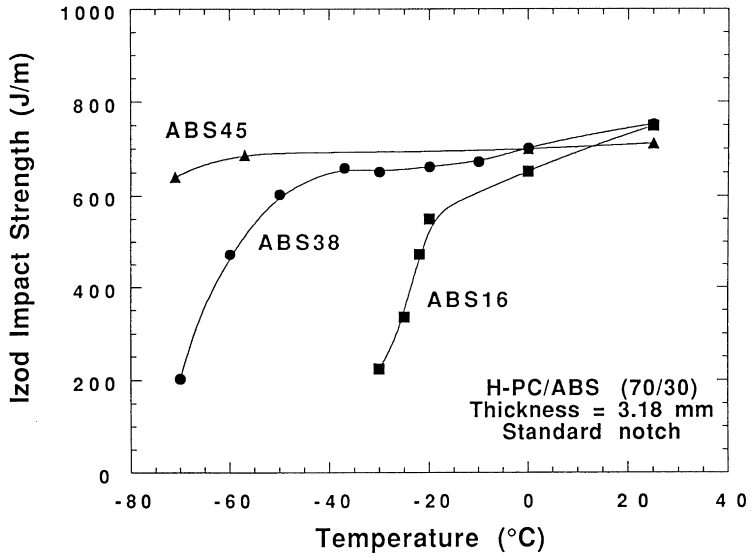

Fig. 9. Izod impact strength of H-PC/ABS (70/30) blends for thin (3.18 mm) samples with a standard notch.

Table 6
Fracture properties of H-PC/ABS38 blends with 16% rubber in the ABS phase

	3.18 mm		6.35 mm			
	Standard notch		Standard notch		Sharp notch	
H-Pc/ABS38 blend	Ductile–brittle transition temperature (°C)	Izod impact Strength (J/m)	Ductile–brittle transition temperature (°C)	Izod impact Strength (J/m)	Plane strain fracture parameters	
					u_0 (KJ/m^2)	u_d (MJ/m^3)
100/0	−40	980	>60	225	4.3	0
70/30	−24	785	10	675	18.7	4.4
50/50	−18	775	−10	440	19.5	3.4
0/100		250	55	65	6.8	0

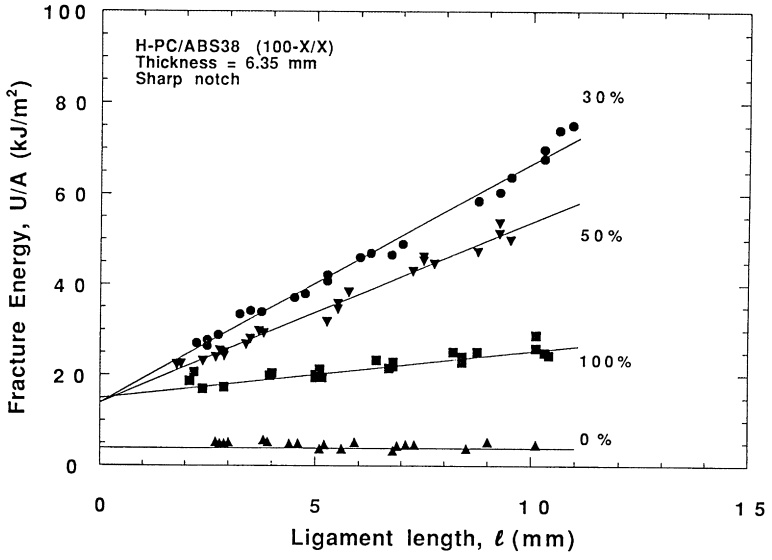

Fig. 10. Dynatup fracture energy for H-PC/ABS38 blends as a function of ligament length for thick (6.35 mm) samples with a sharp notch.

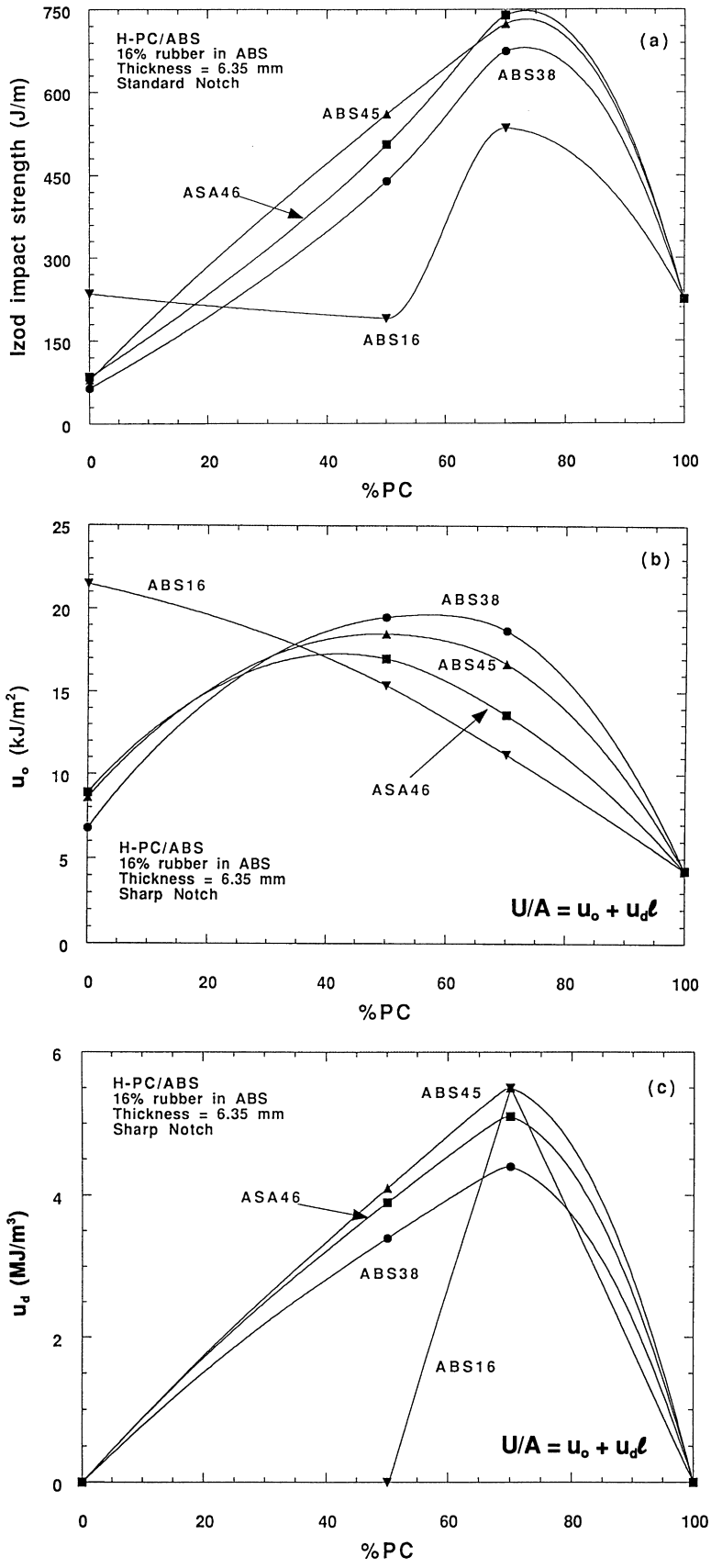

Fig. 11. (a) Izod impact strength, (b) limiting specific fracture energy (u_0), and (c) dissipative energy density (u_d) as a function of blend composition for H-PC/ABS blends with 16% rubber in the ABS phase for thick (6.35 mm) samples.

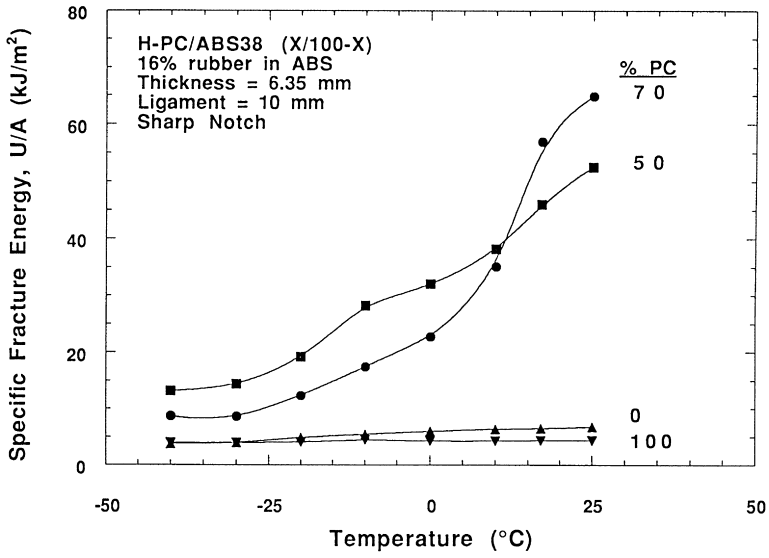

Fig. 12. Dynatup fracture energy (U/A) of H-PC, ABS38 and H-PC/ABS38 blends with 16% rubber in the ABS phase for thick (6.35 mm) samples with a sharp notch and a ligament length of 10 mm.

Table 7
Comparison of PC/ABS and PC/ASA (70/30) blends with 16% rubber in the ABS phase

	3.18 mm		6.35 mm		
	Standard notch		Standard notch	Sharp notch	
Blend (70/30) (16% rubber in ABS)	Ductile–brittle transition temperature (°C)	Izod impact strength (J/m)	Izod impact strength (J/m)	Plane strain fracture parameters	
				u_0 (kJ/m^2)	u_d (MJ/m^3)
H-PC/ABS16	−23	770	535	11.2	5.5
H-PC/ABS38	−24	785	675	18.7	4.4
H-PC/ABS38 (+1%SAN-amine)	−26	775	670	18.9	4.4
H-PC/ABS45	−29	790	725	16.7	5.5
H-PC/ASA46	−24	900	745	13.6	5.1

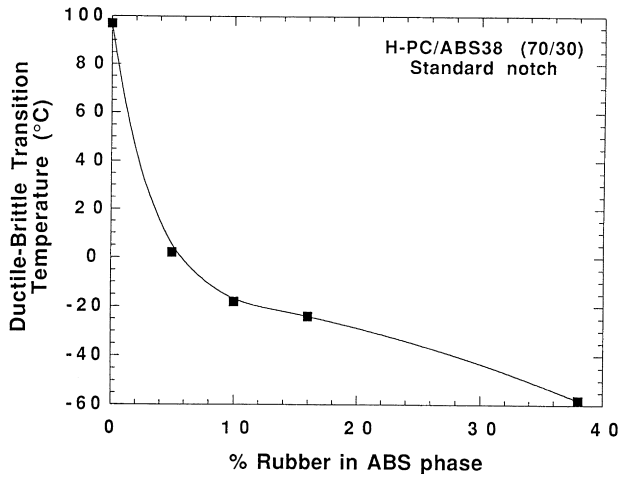

Fig. 13. Ductile–brittle transition temperature as a function of rubber content in the ABS phase for H-PC/ABS38 (70/30) blends using thin (3.18 mm) samples with a standard notch.

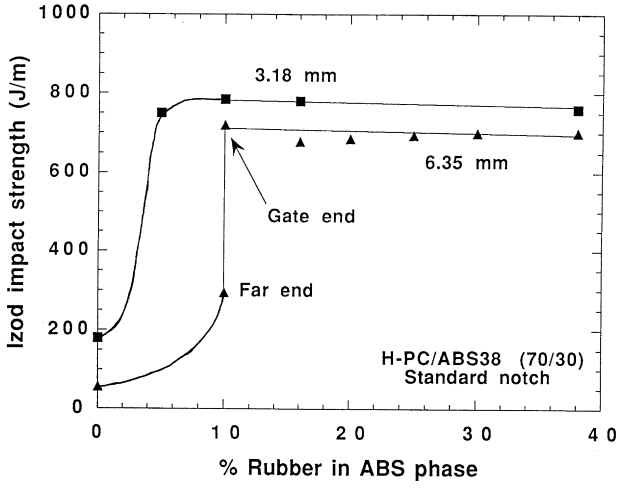

Fig. 14. Izod impact strength as a function of rubber content in the ABS phase for H-PC/ABS38 (70/30) blends using thin (3.18 mm) and thick (6.35 mm) samples a standard notch.

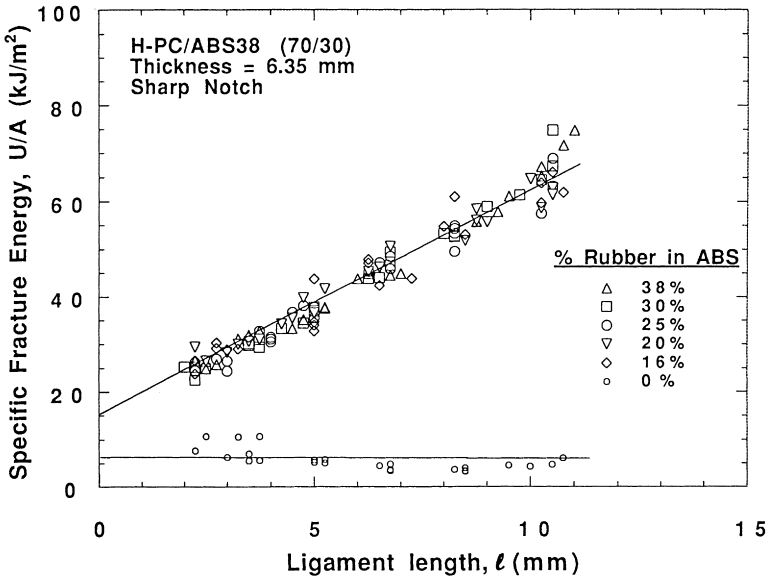

Fig. 15. Fracture energy as a function of ligament length for H-PC/ABS38 (70/30) blends with varying rubber concentrations in the ABS phase for thick (6.35 mm) samples with a sharp notch.

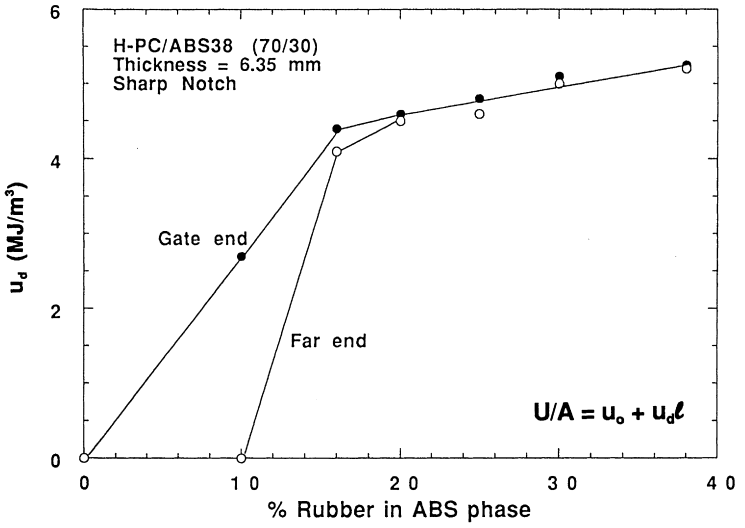

Fig. 16. Dissipative energy density (u_d) of far-end and gate-end specimens (6.35 mm thick, sharp notch) as a function of rubber content in the ABS phase for H-PC/ABS38 (70/30) blends using thick (6.35 mm) samples with a sharp notch.

different ABS and ASA materials used in this study. As previously discussed, each material has a different rubber concentration and morphology. For comparison, two sets of fracture properties are reported for these materials, the as-received materials and these materials diluted with the appropriate SAN to a fixed (16%) rubber concentration. As might be expected, the materials with high rubber contents have somewhat higher Izod impact strength values for both 3.18 and 6.35 mm specimens. The mass produced ABS16 has the highest u_0 while the high rubber content emulsion materials have higher values of u_d. At a fixed rubber content of 16%, only ABS16 shows high values of impact strength for thick samples (6.35 mm) and was the only material to exhibit any stress whitening near the fracture zone.

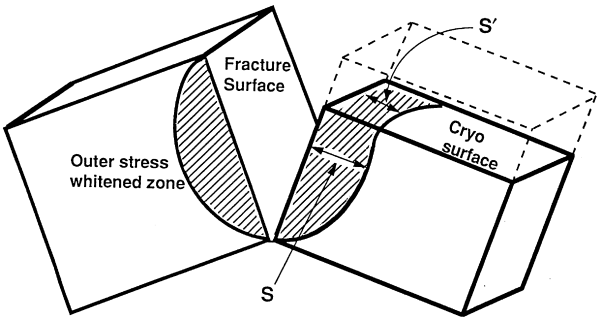

Fig. 17. Schematic of SEN3PB fracture specimen indicating outer, S and inner, S', stress whitened zone sizes measured after cryo-fracturing one half of the sample.

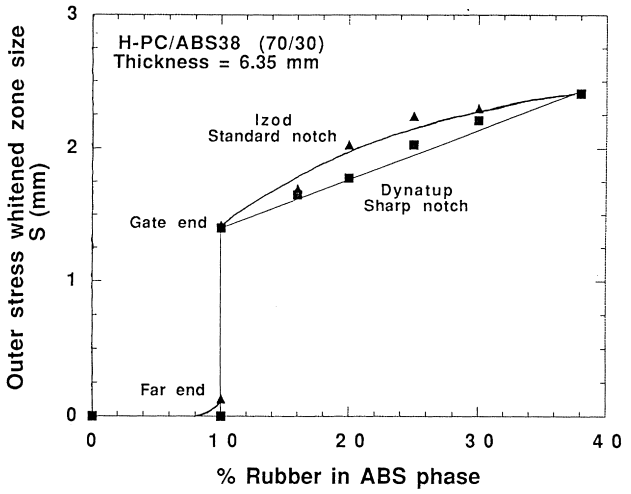

Fig. 18. Outer stress whitened zone size, *S*, as a function of rubber content in the ABS phase for H-PC/ABS38 (70/30) blends using thick (6.35 mm) samples with standard and sharp notches.

Izod impact strength of blends of H-PC with ABS16, ABS38, and ABS 45 using thin (3.18 mm) samples are shown in Fig. 9. While all three blends have similar room temperature impact strength, the blends with higher rubber content ABS materials have superior low temperature toughness compared to the blend with ABS16; the blend of H-PC/ABS45 (70/30) was ductile to −70°C which was the limit of the CO_2 cooling apparatus used in this study. ABS50 was not used for blending with PC because it has been previously shown to severely degrade PC at processing temperature [51].

5.4. Effect of blend composition

The fracture characteristics of H-PC, ABS38 and H-PC/ABS38 blends are shown in Fig. 10 for thick samples (6.35 mm) with sharp notches. Blends of H-PC with 30% and 50% ABS38 exhibited superior toughness at all ligament lengths compared to unblended H-PC and ABS38. However, to effectively compare the extent of toughening provided by different ABS and ASA materials, each material was diluted with SAN to give the same rubber concentration before blending with H-PC. The effect of blend composition on the fracture properties of blends of H-PC with ABS16, ABS38, ABS45 and ASA46 at a fixed rubber content of 16% in the ABS phase are compared in Fig. 11(a)–(c). Fig. 11(a) shows the thick (6.35 mm) specimen Izod impact strength as a function of ABS content in H-PC blends. While 70/30 blends of H-PC with ABS16, ABS45, ABS38, and ASA46 are all super tough, blends with ABS45, ABS38, and ASA46 have superior fracture properties for blends with 50% PC. As seen in Fig. 11(c), very tough blends with corresponding high values of u_d can be produced from H-PC and ABS materials that are brittle or semi-brittle under the test conditions used in this study and have $u_d = 0$. Izod values seem to be more dependent on the slope, u_d, than the intercept, u_0, of U/A versus ℓ plots. However, u_0 does clearly affect impact strength as seen by comparing the various ABS materials shown at 0% PC in Fig. 11(a)–(c).

Addition of ABS38 to H-PC reduced the room temperature Izod impact strength and increased the ductile–brittle transition temperature for thin (3.18 mm) samples, but significantly increased the Izod impact strength, decreased the ductile–brittle transition temperature and increased both u_0 and u_d for thick (6.35 mm) samples. Fig. 12 clearly shows the synergistic effect of blending H-PC with ABS38 containing 16% rubber in the ABS phase. H-PC/ABS38 blends exhibited greater toughness at all temperatures compared to the unblended materials using thick (6.35 mm) samples. A more detailed analysis of the fracture properties of H-PC/ABS38 blends with a fixed rubber

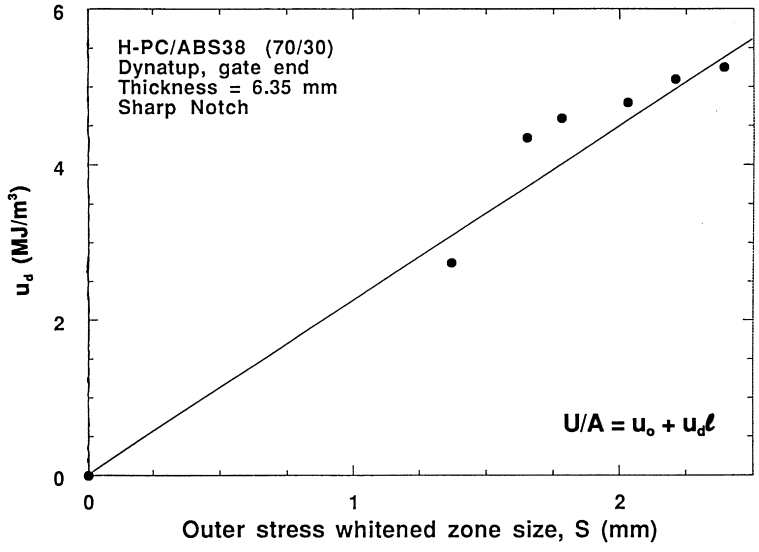

Fig. 19. Dissipative energy density (u_d) versus. outer stress whitened zone size, *S*, using thick (6.35 mm) samples with a sharp notch.

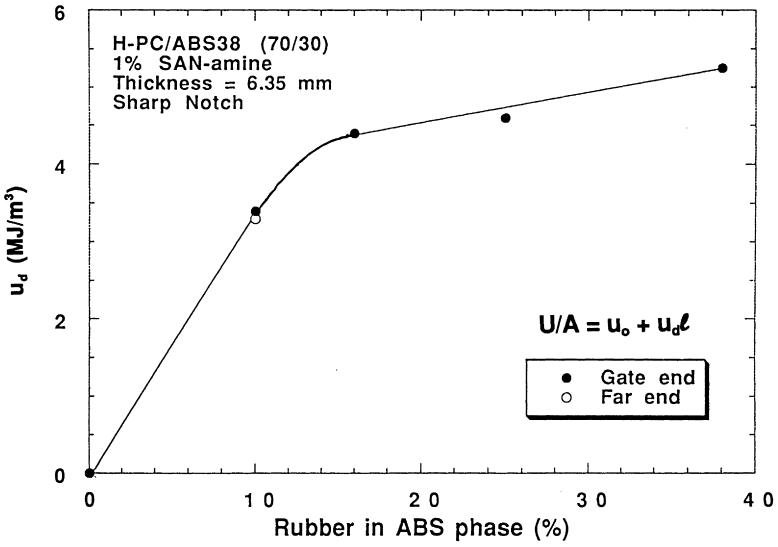

Fig. 20. Dissipative energy density (u_d) as a function of rubber content of the ABS phase for H-PC/ABS38 (70/30) blends with 1% SAN-amine compatibilizer using thick (6.35 mm) samples with a sharp notch.

content of 16% in the ABS phase is summarized in Table 6.

5.5. Effect of ABS type on the fracture properties of PC/ABS (70/30) blends

Table 7 compares the fracture behavior of H-PC blends with different ASA and ABS materials at a fixed blend composition of 70% PC and with a total rubber concentration of 4.8%. To produce a mixture with this rubber concentration, blends of H-PC/ASA and H-PC/ABS with 70% H-PC were diluted with SAN to give a rubber concentration of 16% rubber in the ABS and ASA phase. At this fixed blend composition and rubber content, the emulsion-made ABS and ASA materials exhibit superior toughness when blended with PC. Blends of H-PC with ABS45 at this low total rubber concentration (4.8%) had both the lowest ductile–brittle transition temperature and the highest value of u_d. Blends of ABS16 with H-PC are also very tough; however, this mass-made ABS leads to lower fracture energies for thick specimens compared to blends of ABS38, ABS45, and ASA46 with H-PC. The use of butyl acrylate rubber instead of butadiene rubber in ASA materials significantly improves weatherability but might be expected to result in inferior impact properties under certain conditions because of the higher T_g of the rubber phase. However, the blend of H-PC with ASA46 exhibited the highest impact strength for thin (3.18 mm) samples, similar ductile–brittle transition temperatures as blends of H-PC with ABS, and excellent thick specimen fracture characteristics.

5.6. Effect of rubber content in ABS

The rubber concentration in the ABS phase of H-PC/ABS38 (70/30) blends was varied by pre-blending ABS38 with SAN32.5. Fig. 13 shows that for thin samples with a standard notch increasing the rubber concentration in the ABS phase above the critical rubber concentration (10%) gradually decreases the ductile–brittle transition temperature of the blend. Decreasing the rubber concentration below 10% in the rubber phase significantly increases the ductile–brittle transition temperature to over 60°C for H-PC/SAN32.5 (0% rubber).

Fig. 14 shows that for room temperature toughness there is a critical rubber concentration in the ABS phase. For thick (6.35 mm) samples with a standard notch, this critical rubber concentration was found to be 10% rubber in the ABS phase (3% total rubber in the blend), while thin (3.18 mm) samples with a standard notch were tough even at 5% rubber in the ABS. At the critical rubber concentration for thick samples, the gate end of the specimen exhibited tough behavior with significant stress whitening but the far end of the specimen was only semi-tough and showed areas of brittle fracture. The ductile–brittle behavior for thick specimens is also shown in Fig. 15 by plotting Dynatup fracture energy as a function of ligament length. The slope, u_d, of the U/A versus ℓ plot for H-PC/ABS38 (70/30) as a function of rubber concentration is shown in Fig. 16; this parameter seems closely related to Izod impact strength as u_d is zero until the critical rubber content is reached where there is a step change in value followed by a gradual increase with rubber concentration.

Many tough polymeric materials exhibit a stress whitened zone, which surrounds the fracture surface. The size of this stress whitened zone can be measured perpendicular to the fracture surface; however, the extent of stress whitening in the interior of thick specimens is not necessarily the same as seen on the surface of the sample because of volumetric constraints on the material during loading. In thick specimens like those used here, plane strain conditions tend to

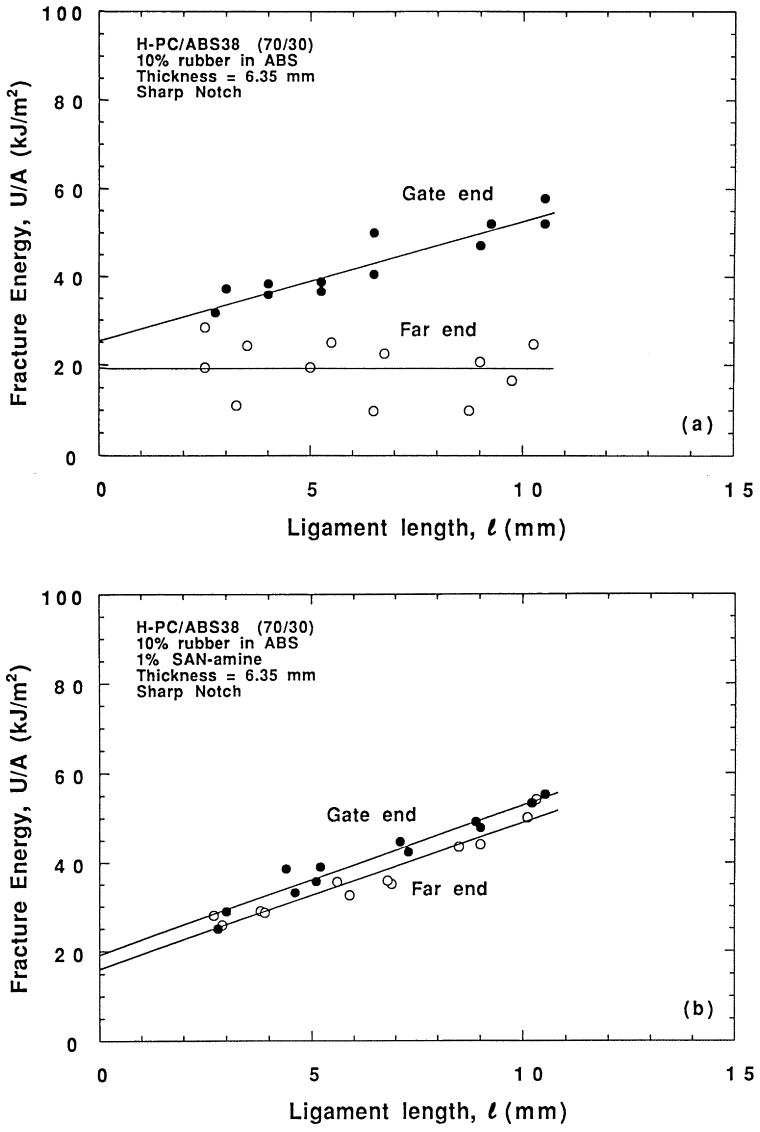

Fig. 21. Fracture energy as a function of ligament length for (a) H-PC/ABS38 (70/30) and (b) H-PC/ABS38 (70/30) using 1% SAN-amine compatibilizer, with 10% rubber in the ABS phase for thick (6.35 mm) samples with a sharp notch.

exist in the interior of the sample while the surface experiences plane stress conditions. The relationship between the outer (S) and inner (S') size of the stress whitened zone is schematically shown in Fig. 17 where one half of the SEN3PB specimen was fractured after cooling in liquid nitrogen to expose the cross-sectional area of the sample. Fig. 18 shows the outer stress whitened zone size (S) as a function of rubber concentration for both standard and sharp notch thick (6.35 mm) samples. The size of the stress whitened zone was measured as the maximum width of the zone perpendicular to the crack on the outer surface of the specimen as shown in Fig. 17. Fig. 18 shows a similar dependence on rubber content as that seen in Figs. 15 and 16 with the same critical rubber concentration (10%). Above 10% rubber, the stress whitened zone size increases almost linearly with rubber concentration, while the impact strength and u_d are relatively independent of rubber content in this range. These seemingly contrary observations can be explained by the fact that while the outer stress whitened zone size (S) increases, the inner size of the zone (S') is nearly constant for rubber concentrations greater than 10%. Therefore, both the fracture energy and the total volume of stress whitened material change only nominally above the critical rubber concentration. The relationship between these parameters is shown in Fig. 19 with a linear dependence of u_d on the outer stress whitened zone size of thick (6.35 mm) Izod specimens.

5.7. Effect of reactive compatibilization

Comparison of Figs. 20 and 16 shows that incorporation of 1% SAN-amine in a 70/30 blend of H-PC/ABS38 significantly improves the fracture toughness of the far end of the injection molded sample. The difference in fracture

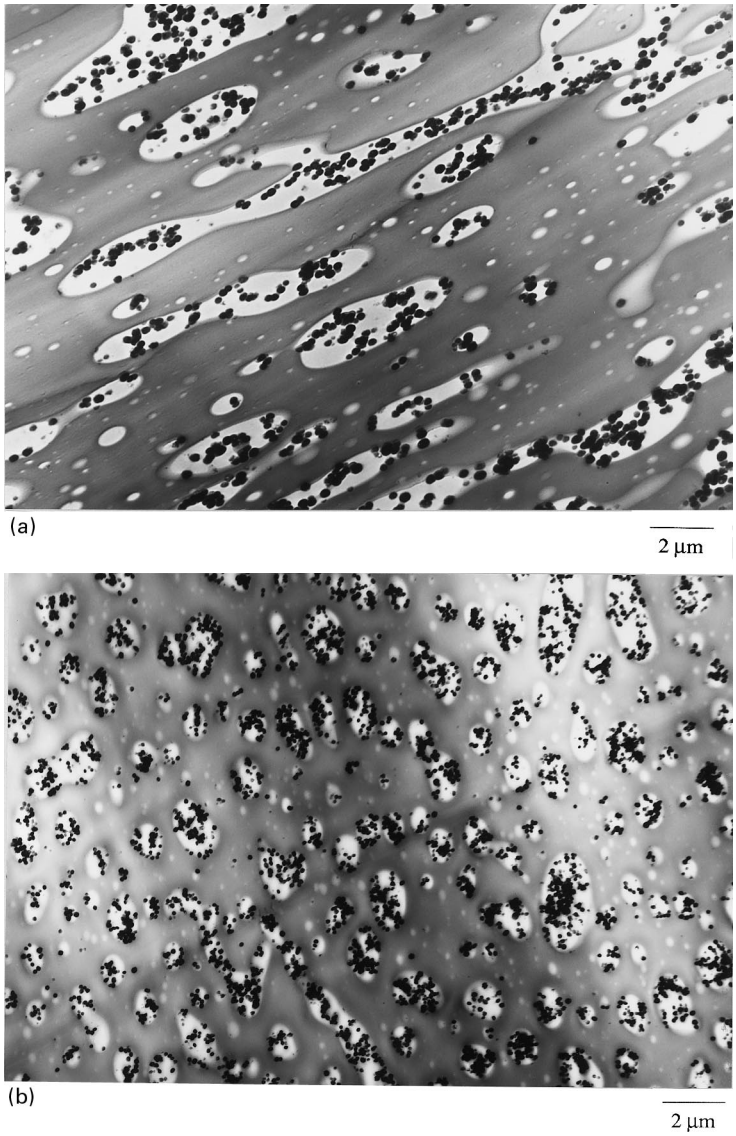

Fig. 22. TEM photomicrographs showing the morphology of the (a) far-end and (b) gate-end of injection molded bars for uncompatibilized H-PC/ABS38 (70/30) blends with 10% rubber in the ABS compared to (c) far end and (d) gate-end of H-PC/ABS38 (70/30) blends with 10% rubber in the ABS compatibilized using 1% SAN-amine.

properties between the far and gate ends of thick (6.35 mm) samples for blends with 10% rubber in the ABS phase is seen in Fig. 21(a) and (b). This difference was thought to be the result of morphological rearrangements in the mold during the filling and cooling cycles. The effect of reactive compatibilization using the previously described SAN-amine polymer on the morphology development and stability of PC/SAN was examined in two previous articles [43,44]. Although compatibilized and uncompatibilized blends exhibited similar morphologies and properties for thin (3.18 mm) samples, there were significant differences for thick injection molded specimens. Figs. 22(a)–(d) show the dramatic difference between the morphology of the far ends of the injection molded 6.35 mm samples for compatibilized and uncompatibilized H-PC/ABS38 at the critical rubber concentration (10% in the ABS phase). The ABS phase was well dispersed in the thin samples and the gate-end of the thick samples as shown in Fig. 22(b). This suggests that ABS can be well dispersed in PC without the aid of a compatibilizer, but the poor dispersion seen in Fig. 22(a) results from the morphological instability of uncompatibilized PC/ABS blends. The morphology of the compatibilized blend is much more stable.

6. Conclusions

The fracture of thin (3.18 mm) and thick (6.35 mm) specimens of PC, ABS and PC/ABS blends with both standard and sharp notches was examined by standard Izod and single edge notch three point bend (SEN3PB) instrumented Dynatup tests. Ligament lengths were varied for SEN3PB

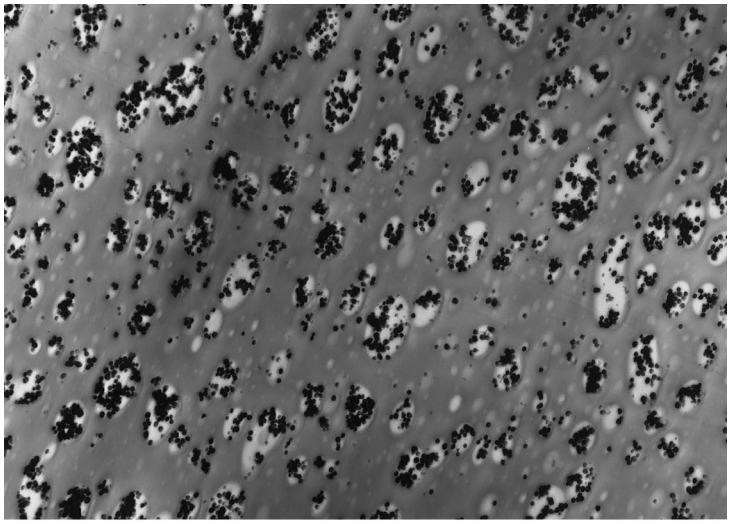

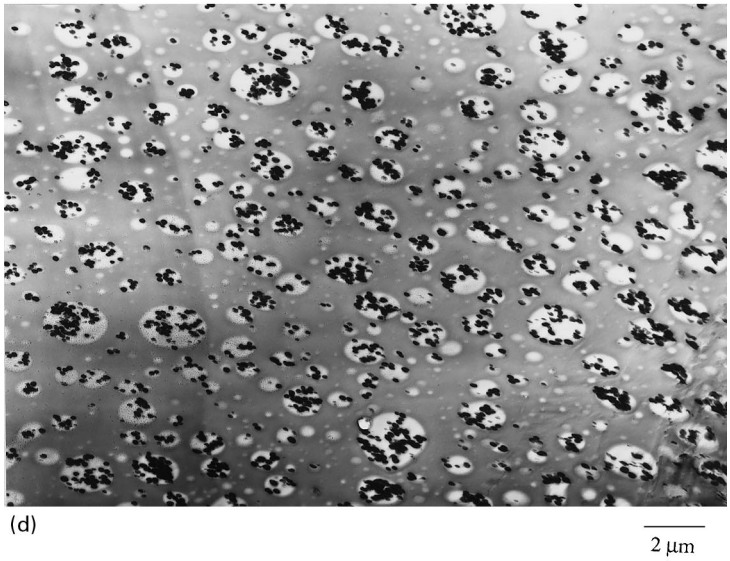

Fig. 22. (*continued*)

samples and the corresponding fracture data were represented by plotting the specific fracture energy (U/A) as a function of ligament length (ℓ). Blends of PC with ABS or acrylate–styrene–acrylonitrile (ASA) were found to be super tough for thick and thin samples with both standard and razor notches. These blends had higher fracture energy values at zero ligament length, intercept $= u_0$, and dissipative energy densities, slope $= u_d$, compared to either PC or ABS materials. Neat PC materials with higher molecular weight have larger intercepts but they remain independent of ligament length, i.e., the slope or u_d remains 0. For PC/ABS (70/30) blends, a critical rubber concentration of 10% in the ABS phase (3% total rubber in the blend) was found where the far-end of thick (6.35 mm) injection molded bars were brittle ($u_d = 0$) and the gate-end was tough ($u_d > 0$); u_d increased with increasing rubber content above this critical value.

The incorporation of 1% of an SAN-amine compatibilizer produced tough samples for both far and gate-end samples at the same rubber concentration. TEM analysis of the blend morphology confirmed that the lowered fracture toughness in the far-end of the uncompatibilized specimens was because of the formation of large ABS domains caused by coalescence during the injection molding cycle; both the gate and far-end of the compatibilized blend had small, well dispersed ABS domains. Izod impact energy and u_d were shown to be directly proportional to the stress whitened zone size surrounding the fracture surface of the samples. The presence of a stress whitened zone seems to be a necessary but not sufficient requirement for a material to exhibit a significant u_d; there were some blends with a stress whitened zone but $u_d = 0$, while there were no blends with a positive u_d without a stress whitened zone.

Acknowledgements

This research was supported by the US Army Research Office. Various polymers used in this work were supplied by Bayer Corporation, Cheil Industries, The Dow Chemical Company, GE Plastics, Mitsubishi Engineering Plastics Corporation and Sumitomo Chemical. The authors are grateful to Clive Bucknall for his helpful discussions and insight. The authors would also like to thank Allen Padwa of Bayer Corporation for his contributions in this work.

References

[1] Lombardo BS, Keskkula H, Paul DR. J Appl Polym Sci 1994;54:1697.
[2] Quintens D, Groeninckx G, Guest M, Aerts L. Polym Eng Sci 1990;30:1474.
[3] Wu J, Shen S, Chang F. J Appl Polym Sci 1993;50:1379.
[4] Riew CK, Smith RW. Rubber-toughened plastics. In: Riew CK, editor. ACS symposium series, 222. New Orleans, LA: American Chemical Society, 1989.
[5] Ishikawa M, Chiba I. Polymer 1990;31:1232.
[6] Kurauchi T, Ohta T. J Mater Sci 1984;19:1699.
[7] Grabowski TS. US Pat. 3,130,177 (1964) (to Borg-Warner Corporation).
[8] Greco R, Sorrentino A. Adv Polym Tech 1994;13:249.
[9] Greco R. In: Martuscelli E, Musto P, Ragosta G, editors. Advanced routes for polymer toughening, vol. 10. In: Jenkins AD, editor. Polymer Science Library, ch. 9. Amsterdam: Elsevier, 1996.
[10] Santana OO, Maspoch ML, Martinez AB. Polym Bull 1997;39:511.
[11] Ishikawa M. Polymer 1995;36:2203.
[12] Lu M, Chiou K, Chang F. Polym Eng Sci 1996;36:2289.
[13] Seidler S, Grellmann W. J Mater Sci 1993:4078.
[14] Lu M, Chiou K, Chang F. Polymer 1996;37:4289.
[15] Lu M, Chiou K, Chang F. J Appl Polym Sci 1996;62:863.
[16] Mai Y. Polym Comm 1989;30:330.
[17] Paton CA, Hashemi S. J Mater Sci 1992;27:2279.
[18] Heino M, Hietaoja P, Seppala J, Harmia T, Friedrich K. J Appl Polym Sci 1997;66:2209.
[19] Levita G, Parisi L, Mcloughlin S. J Mater Sci 1996;31:1545.
[20] Levita G, Parisi L, Marchetti A. J Mater Sci 1994;29:4545.
[21] Wu J, Mai Y. Polym Eng Sci 1996;36:2275.
[22] Pegoretti A, Marchi A, Ricco T. Polym Eng Sci 1997;37:1045.
[23] Partridge I, Sanz C, Bickerstaff K. Polymer processing society. Fifth Annual Meeting, Kyoto, 1989.
[24] Mamat A, Vu-Khanh T, Favis BD. J Polym Sci 1997;35:2583.
[25] Vu-Khanh T. Polymer 1988;29:1979.
[26] Vu-Khanh T. Theor Appl Fract 1994;21:83.
[27] Kayano Y, Keskkula H, Paul DR. Polymer 1997;38:1885.
[28] Kayano Y, Keskkula H, Paul DR. Polymer 1998;39:821.
[29] Broberg KB. Int J Fract 1968;4:11.
[30] Mai Y. Int J Mech Sci 1993;35:995.
[31] Mai Y, Williams JG. J Mater Sci 1977;12:1376.
[32] Gonzalez-Montiel A, Keskkula H, Paul DR. Polymer 1995;36:4605.
[33] Majumdar B, Keskkula H, Paul DR. Polymer 1994;35:3164.
[34] Oshinski AJ, Keskkula H, Paul DR. Polymer 1992;33:268.
[35] Triacca VJ, Ziaee S, Barlow JW, Keskkula H, Paul DR. Polymer 1991;32:1401.
[36] Thakkar AN, Grossman SJ. Soc Plast Eng ANTEC 1991:647.
[37] Duvall J, Sellitti C, Topolkaraev V, Hiltner A, Baer E, Myers C. Polymer 1994;35:3948.
[38] Kim BK, Lee YM, Jeong HM. Polymer 1993;34:2075.
[39] Ide F, Hasegawa A. J Appl Polym Sci 1974;18:963.
[40] Lavengood RE, Padwa AR, Harris AF. US Pat. 4,713,415 (1987) (to Monsanto).
[41] Lavengood RE, Silver FM. Soc Plast Eng ANTEC 1987;45:1369.
[42] Wildes GS, Harada T, Keskkula H, Janarthanan V, Padwa AR, Paul DR. Submitted to Polymer.
[43] Wildes GS, Keskkula H, Paul DR. Submitted to Polymer.
[44] Wildes GS, Keskkula H, Paul DR. Submitted to J Polym Sci Part B: Polym Phys.
[45] Partridge I. In: Miles IS, Rostami S, editors. Multicomponent polymer systems, Essex: Longman Scientific, 1992 ch. 5.
[46] Vitali R, Montani E. Polymer 1980;21:1220.
[47] Plati E, Williams JG. Polym Eng Sci 1975;15:470.
[48] Singh RK, Parihar KS. J Mater Sci 1986;22:2503.
[49] McCrum NG, Buckley CP, Bucknall CB. Principles of polymer engineering ch. 5. Oxford: Oxford University Press, 1988.
[50] Parvin M, Williams JG. Int J Fract 1975;11:963.
[51] Lombardo MS. Thesis, University of Texas, 1994.